

# Joint PHD Filter and Hungarian Assignment Algorithm for Multitarget Tracking in Low Signal-to-Noise Ratio

Shanzhu XIAO, Huamin TAO, Xinglin SHEN\*, Luping ZHANG, Moufa HU

National Key Laboratory of Science and Technology on ATR, College of Electronic Science,  
National University of Defense Technology, Changsha 410073, China

mountbamboo@vip.163.com, taohmpeach@163.com, xlshencom@163.com, zhangluping-002@163.com,  
hu199709\_200106@sina.com

Submitted January 5, 2023 / Accepted May 9, 2023 / Online first May 17, 2023

**Abstract.** *Multitarget tracking (MTT) for image processing in low signal-to-noise ratio (SNR) is difficult and computationally expensive because the distinction between the target and the background is small. Among the current MTT algorithms, Random Finite Set (RFS) based filters are computationally tractable. However, the probability hypothesis density (PHD) filter, despite its low computational complexity, is not suitable for MTT in low SNR. The generalized labeled multi-Bernoulli (GLMB) filter and its fast implementation are unsuitable for realtime MTT due to their high computational complexity. To achieve realtime MTT in low SNR, a joint PHD filter and Hungarian assignment algorithm is first proposed in this work. The PHD filter is used for preliminary tracking of targets while the Hungarian assignment algorithm is employed to complete the association process. To improve the tracking performance in low SNR, a new track must undergo a trial period and a valid track will be terminated only if it is not detected for several frames. The simulation results show that the proposed MTT algorithm can achieve stable tracking performance in low SNR with small computational complexity. The proposed filter can be applied to MTT in low SNR that require realtime implementation.*

## Keywords

Hungarian assignment algorithm, PHD filter, multitarget tracking (MTT), low signal-to-noise ratio (SNR)

## 1. Introduction

Multitarget tracking (MTT) at a low signal-to-noise ratio (SNR) is an important subject for image processing [1]. Traditionally, measurements are obtained through a thresholding process. In scenarios with high SNR, information loss incurred during threshold segmentation has a negligible impact on tracking performance because of a high detection probability while minimizing false alarms [2], [3]. However, in scenarios with low SNR, distinguishing targets from the

background is more challenging, and information loss can negatively impact tracking performance. Additionally, maintaining a high detection probability in low SNR scenarios increases the number of false alarms.

Track-before-detect (TBD) algorithms [4–8] have been proposed as means of enhancing tracking performance in low SNR situations. However, the computational complexity of these algorithms is generally so great that they cannot be implemented in real time. Similarly, MTT algorithms using the target amplitude to obtain better performance also have high computational complexity [9], [10]. Classical MTT algorithms [11], [12] demand extensive computation and storage, and the realtime tracking performance is not ideal. Simultaneously, in low SNR, they are also poor in handling the missed detection of the target or a large number of false alarms. Using the Finite Set Statistics (FISST) framework [13], [14], a set of Random Finite Set (RFS) based filters have been developed to facilitate MTT as they are computationally tractable. The probability hypothesis density (PHD) filter [15–17], which propagates the first moment to approximate the multitarget probability density function (PDF), makes it ideal for realtime implementation with its low computational complexity. However, because too much information is discarded, when dealing with a high occurrence of false alarms, the classic PHD filter may not be the best choice. Similarly, the labeled PHD filters [18], [19] primarily serve to enhance the identification of distinct targets, rather than bolstering tracking performance under low SNR conditions. Currently, the PHD filter that can be applied to low SNR has not been studied except for a PHD filter with low detection probability [20]. Based on the generalized labeled multi-Bernoulli (GLMB) RFS [21], the  $\delta$ -GLMB filter [22], [23] is a provable Bayes optimal tracking filter. Although it has good tracking performance, the  $\delta$ -GLMB filter and its fast implementation [24], [25] cannot easily be applied to realtime scenarios because its computational complexity is high.

Simple online and realtime tracking (SORT) [26] is a simple framework for video object tracking that uses a Kalman filter and Hungarian assignment algorithm [27], achieving favorable MTT performance by utilizing the

frame-by-frame data association with a cost metric calculated from the bounding box. Researchers have also proposed SORT with a deep association metric (deep-SORT) [28] to achieve a more stable target state. However, in low SNR, the targets might not exhibit any discernible shape, making it unfeasible to obtain a bounding box. Achieving detection probability assurance in such cases might necessitate a high number of thresholding measurements and escalate the computational complexity of data association. Thus, the SORT and deep-SORT might not be ideally suited for MTT in low SNR. At present, there are no good solutions for multitarget fast tracking for low SNR.

In this work, to achieve realtime MTT in low SNR, a joint PHD filter and Hungarian assignment algorithm is proposed for the first time in our work. We begin by using the PHD filter to obtain the preliminary target state, followed by the Hungarian algorithm to complete target association and obtain tracks. The algorithm maintains target tracking performance in low SNR by keeping tracks alive even when the PHD filter fails to update their state. The simulation results show that the proposed algorithm and the GLMB filter have similar tracking performance in low SNR. The computation time of the proposed algorithm has almost no increase compared with the PHD filter. Overall, the algorithm proposed in this paper is a high-performance target tracking algorithm that can be implemented easily.

The structure of the remaining part of the paper is as follows: Section 2 introduces the research background. Section 3 introduces the joint PHD filter and Hungarian assignment algorithm. Section 4 presents the simulation results of the joint PHD filter and Hungarian assignment algorithm. Section 5 is the conclusion.

## 2. Background

### 2.1 Multitarget Bayesian Filter and Random Finite Set

Given a time-sequence measurement set  $Z_{1:k}: Z_1, \dots, Z_k$ , the recursion of the multitarget Bayesian filter [14] at frame  $k$  can be expressed as

$$\dots \rightarrow f(X_{k-1} | Z_{1:k-1}) \rightarrow f(X_k | Z_{1:k-1}) \rightarrow f(X_k | Z_{1:k}) \rightarrow \dots \quad (1)$$

where  $f(X_{k-1} | Z_{1:k-1})$  is the prior multitarget PDF (the posterior PDF at frame  $k-1$ ),  $f(X_k | Z_{1:k-1})$  is the predicted multitarget PDF, and  $f(X_k | Z_{1:k})$  is the posterior multitarget PDF (the prior PDF at frame  $k+1$ ).

The process of calculating  $f(X_k | Z_{1:k-1})$  from  $f(X_{k-1} | Z_{1:k-1})$  is called the predictor, also called the time update. The predictor is

$$f(X_k | Z_{1:k-1}) = \int f(X_k | X_{k-1}) \cdot f(X_{k-1} | Z_{1:k-1}) \delta X_{k-1} \quad (2)$$

where  $f(X_k | X_{k-1})$  is the multitarget state-transition function.

The process of calculating  $f(X_k | Z_{1:k})$  from  $f(X_k | Z_{1:k-1})$

is called the corrector, also called the measurement update. The corrector is

$$f(X_k | Z_{1:k}) = \frac{f(Z_k | X_k) \cdot f(X_k | Z_{1:k-1})}{\int f(Z_k | X_k) \cdot f(X_k | Z_{1:k-1}) \delta X_k} \quad (3)$$

where  $f(Z_k | X_k)$  is the sensor multitarget PDF.

In the framework of RFS, the multitarget state set and the measurement set are represented as RFS  $X = \{\mathbf{x}_1, \mathbf{x}_2, \dots, \mathbf{x}_n\}$  and  $Z = \{z_1, z_2, \dots, z_m\}$ , where  $n$  is the target number and  $m$  is the measurement number.

The PHD  $D(\mathbf{x})$ , which is the first moment approximation of the multitarget PDF  $f(X)$  [14], and the probability generating functional (PGFL)  $G[h]$  play important roles in the RFS based filters. The PGFL is defined as

$$G[h] = \int h^X f(X) \delta X \quad (4)$$

where  $h^X$  is the power functional defined by  $h^X = \prod_{\mathbf{x} \in X} h(\mathbf{x})$  if  $X \neq \emptyset$  and  $h^X = 1$  otherwise.

The PHD  $D(\mathbf{x})$  can be calculated as

$$D(\mathbf{x}) = \frac{\delta G[1]}{\delta \mathbf{x}}. \quad (5)$$

### 2.2 PHD Filter

The PHD filter [15–17], which is a multitarget Bayesian filter in the framework of RFS, propagates the PHD to approximate the multitarget PDF. Given a time-sequence measurement sets  $Z_{1:k}: Z_1, \dots, Z_k$ , the recursive of the PHD filter at frame  $k$  can be expressed as

$$\dots \rightarrow D_{k-1|k-1}(\mathbf{x}) \rightarrow D_{k|k-1}(\mathbf{x}) \rightarrow D_{k|k}(\mathbf{x}) \rightarrow \dots \quad (6)$$

where the prior PHD  $D_{k-1|k-1}(\mathbf{x})$  is used to approximate  $f(X_{k-1} | Z_{1:k-1})$ , the predicted PHD  $D_{k|k-1}(\mathbf{x})$  is used to approximate  $f(X_k | Z_{1:k-1})$ , and the posterior PHD  $D_{k|k}(\mathbf{x})$  is used to approximate  $f(X_k | Z_{1:k})$ .

The predictor of the PHD filter is

$$D_{k|k-1}(\mathbf{x}) = \int \phi_{k|k-1}(\mathbf{x}, \mathbf{x}_{k-1}) D_{k-1|k-1}(\mathbf{x}_{k-1}) d\mathbf{x}_{k-1} + \eta_k(\mathbf{x}), \quad (7)$$

$$\phi_{k|k-1}(\mathbf{x}, \mathbf{x}_{k-1}) = b_{k|k-1}(\mathbf{x} | \mathbf{x}_{k-1}) + p_s(\mathbf{x}_{k-1}) f_{k|k-1}(\mathbf{x} | \mathbf{x}_{k-1}) \quad (8)$$

where  $\eta_k(\mathbf{x})$  and  $b_{k|k-1}(\mathbf{x} | \mathbf{x}_{k-1})$  represent the PHD of the newborn target and the spawn target,  $p_s(\mathbf{x}_{k-1})$  and  $f_{k|k-1}(\mathbf{x} | \mathbf{x}_{k-1})$  represent the target survival probability and the Markov transition density of the survival target, respectively.

The state transition equation can be expressed as

$$\mathbf{x}_k = F\mathbf{x}_{k-1} + \mathbf{w}_k \quad (9)$$

where  $F$  denotes the state transition matrix and  $\mathbf{w}_k$  denotes the process noise. Then the Markov transition density can be

expressed as

$$f_{k|k-1}(\mathbf{x}_k | \mathbf{x}_{k-1}) = f_{\mathbf{w}_k}(\mathbf{x}_k - F\mathbf{x}_{k-1}) \quad (10)$$

where  $f_{\mathbf{w}_k}(\cdot)$  is the PDF of the noise  $\mathbf{w}_k$ .

If the clutter process can be modelled by a Poisson RFS with mean  $\lambda$  and spatial distribution  $c(\mathbf{z})$ , the corrector is

$$D_{k|k}(\mathbf{x}) = L_{Z_k}(\mathbf{x}) \cdot D_{k|k-1}(\mathbf{x}), \quad (11)$$

$$L_{Z_k}(\mathbf{x}) = 1 - p_D(\mathbf{x}) + \sum_{z \in Z_k} \frac{p_D(\mathbf{x}) \Phi_z(\mathbf{x})}{\lambda c(\mathbf{z}) + D_{k|k-1}[p_D \Phi_z]}, \quad (12)$$

$$D_{k|k-1}[h] = \int h(\mathbf{x}) D_{k|k-1}(\mathbf{x}) d\mathbf{x} \quad (13)$$

where  $p_D(\mathbf{x})$  represents the detection probability of the target, and  $\Phi_z(\mathbf{x}) = f_k(z|\mathbf{x})$  represents the sensor observation likelihood function.

If the measurement model is

$$\mathbf{z} = h(\mathbf{x}) + \mathbf{e} \quad (14)$$

then the measurement likelihood function is

$$f_k(\mathbf{z} | \mathbf{x}) = f_e(\mathbf{z} - h(\mathbf{x})) \quad (15)$$

where  $\mathbf{e}$  is the measurement noise,  $f_e(\cdot)$  is the PDF of the noise  $\mathbf{e}$ . The function  $h(\mathbf{x})$  denotes the sensor measurement functions.

The expected number of targets is

$$N_{k|k} = \text{round}\left(\int D_{k|k}(\mathbf{x}) d\mathbf{x}\right). \quad (16)$$

Multiple target state estimates can be derived from the posterior PHD by finding the  $N_{k|k}$  largest local extreme points  $\hat{\mathbf{x}}_1, \dots, \hat{\mathbf{x}}_n$  of  $D_{k|k}(\mathbf{x})$ . These are the multiple target state estimates at frame  $k$ .

The PHD filter propagates the PHD to approximate the multitarget PDF, which will cause too much information discarded. Therefore, using the classical PHD filter for MTT with a large number of false alarms may not be ideal. Despite its drawbacks, the PHD filter remains the filter with the lowest computational complexity among all RFS based filters and is therefore favored for real-time implementation.

Due to the multidimensional integrals involved in the calculation of the PHD filter, some computationally feasible approximation implementation techniques are necessary. Among these, Sequential Monte Carlo (SMC) and Gaussian mixture (GM) implementations have gained popularity, resulting in the SMC-PHD filter [16] and the GM-PHD filter [17], respectively. Compared to the SMC-PHD filter, the GM-PHD filter has lower computational complexity.

### 2.3 Hungarian Assignment Algorithm

The Hungarian assignment algorithm [27], also known as the Kuhn-Munkres algorithm, is an algorithm for finding the largest weighted assignment in a bipartite graph. The

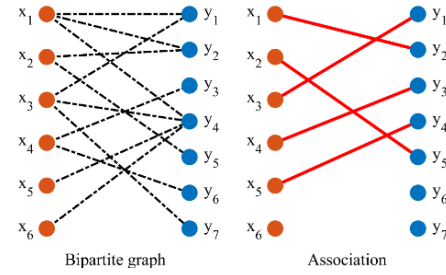


Fig. 1. Bipartite graph and the association of Hungarian assignment algorithm.

Hungarian assignment algorithm plays an important role in the data association of MTT.

In the SORT algorithm, the role of the Hungarian assignment algorithm is to assign the track predicted by the Kalman filter to the detection in the current frame. Essentially, it searches for the best match between multiple targets in the two frames before and after. Assuming that  $n$  targets are detected in the current frame, the Kalman filter performs state prediction on the  $m$  tracks in the previous frame, and the cost matrix is  $C_{nm}$  obtained by calculating the similarity. The Hungarian assignment algorithm solves the cost matrix to obtain the optimal assignment between the detection target and the predicted trajectory to achieve the association of the target in the two frames before and after. The association includes the assigned tracks, the unassigned tracks, and the unassigned detections. The sum of the numbers of assigned tracks and unassigned detections is the target number  $n$ . The sum of the numbers of assigned tracks and unassigned tracks is the track number  $m$ .

Assuming that the detections in the current frame are denoted by  $X = \{x_1, x_2, x_3, x_4, x_5, x_6\}$ , the state prediction of the tracks in the previous frame are denoted by  $Y = \{y_1, y_2, y_3, y_4, y_5, y_6, y_7\}$ . A bipartite graph and the association are shown in Fig. 1. The detailed process of the Hungarian assignment algorithm can be found in [27]. In the figure,  $\{(x_1, y_2), (x_2, y_5), (x_3, y_1), (x_4, y_3), (x_5, y_4)\}$  are the assigned tracks,  $x_6$  is the unassigned detection, and  $y_6, y_7$  are the unassigned tracks.

### 2.4 Analysis of the Low SNR Measurement Set

The image considered in this work is a common observation model defined as follows. The two-dimensional observation image consists of an array of pixels with scalar magnitude values. Suppose that the observation image is a  $A_{\text{pixel}} \times B_{\text{pixel}}$  array, and the index of each pixel is treated as an ordered pair of integers  $i = (a, b)$ , where  $1 \leq a \leq A$ ,  $1 \leq b \leq B$ . The observation image is then given by the PDF of the magnitude value of the pixel. A target with state  $\mathbf{x}$  illuminates the pixels whose center is closest to the position of the target. Given a state  $\mathbf{x}$ , the PDF of the magnitude value  $z_i$  of pixel  $i$  is a Gaussian density defined as follows:

$$\varphi_i(z_i | \mathbf{x}) = \mathcal{N}(z_i; h_i(\mathbf{x}), \sigma^2) \quad (17)$$

where  $h_i(\mathbf{x})$  is the mean and  $\sigma^2$  is the variance.  $h_i(\mathbf{x})$  repre-

sents the contribution of the value  $z_i$  from the state  $\mathbf{x}$  to pixel  $i$ . In the regions of influence of the target,  $h_i(\mathbf{x})$  is a positive value determined by the distance. Outside the regions of influences of the target,  $h_i(\mathbf{x}) = 0$ , the PDF of the magnitude value  $z_i$  of pixel  $i$  is a zero-mean Gaussian density defined as follows:

$$\varphi_i(z_i) = \mathcal{N}(z_i; 0, \sigma^2). \tag{18}$$

If the region of influence of the target is a point, the target is a point target. Statistically, the magnitude value of the location with the target will be greater than that of the location without the target. The SNR is defined as

$$SNR = \frac{\max h_i(\mathbf{x})}{\sigma}. \tag{19}$$

In each frame, the measurement set for the PHD filter can be obtained from the image using a threshold. When the SNR is high, the pixels with targets are significantly different from the pixels without targets. Thus, a high target detection probability can be obtained with a small number of false alarms by using a high threshold. Figure 2(a) shows an image with  $SNR = 6$ . Due to the high SNR, it is easy to distinguish four brighter points in the image. Figure 2(b) shows the thresholding measurement set when the false alarm rate is  $p_f = 10^{-5}$ . As seen from the figure, there are only four thresholding measurements at this time, which do not contain any false alarms. It should be pointed out that this is an ideal situation, and there is a small possibility of false alarms and missed detections when the SNR is high. Since the number of false alarms to be processed is small and the continuity of the target measurements is good, the target tracking algorithm can achieve good tracking performance.

When the SNR is low, a low target detection probability would be obtained with a small number of false alarms by using a high threshold, while a higher target detection probability would be obtained with a large number of false alarms by using a small threshold. Figure 3(a) shows an image with  $SNR = 4$ . Due to the low SNR, it is difficult to distinguish four brighter points in the image. Figure 3(b) shows the thresholding measurement set when the false alarm rate is  $p_f = 10^{-5}$ . As seen from the figure, there is only 1 thresholding measurement at this time and the other 3 target measurements are missed. Figure 3(c) shows the thresholding measurement set when the false alarm rate is  $p_f = 10^{-4}$ . As seen from the figure, there are 3 thresholding measurements at this time and the other target measurements are missed. Figure 3(d) shows the thresholding measurement set when the false alarm rate is  $p_f = 10^{-3}$ . As seen from the figure, there are 3 target measurements as well as 4 false alarms at this time. Therefore, a higher detection probability means more false alarms. It is almost impossible to obtain a high detection probability with low false alarms using only a single frame of a low SNR image. However, both a low target detection probability and a high number of false alarms will result in poor tracking performance. Therefore, how to achieve effective target tracking under a low SNR is of great significance.

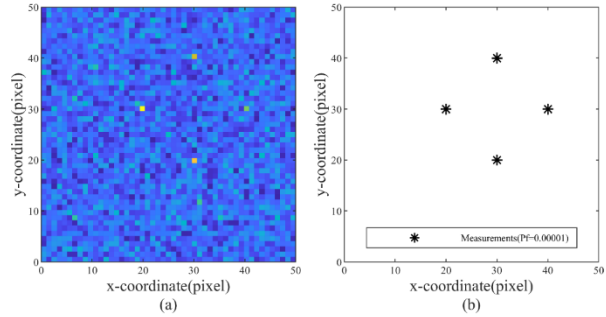


Fig. 2. Image and measurement set with SNR = 6.

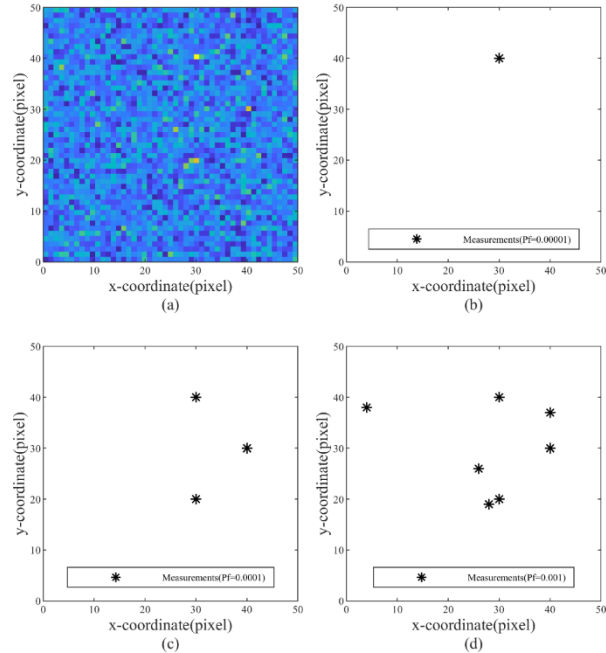


Fig. 3. Image and measurement set with SNR = 4.

### 3. Joint PHD Filter and Hungarian Assignment Algorithm

#### 3.1 Algorithm Framework

A joint PHD filter and Hungarian assignment algorithm is proposed in our work. First, the image is pre-processed with a low threshold, and a measurement set with a high number of false alarms is generated. This measurement set is then fed into the PHD filter to complete the target tracking to obtain the preliminary target states. Then the cost matrix for assignment is selected as the Euclidean distance between the predicted tracks of the last frame and the preliminary target states at the current frame. The assignment is solved by using the Hungarian assignment algorithm with the cost matrix. Finally, the tracks are updated according to the result of the assignment.

To prevent any incorrect tracking, the algorithm mandates a trial period for newly created tracks. During this period, the track must align with the preliminary target state

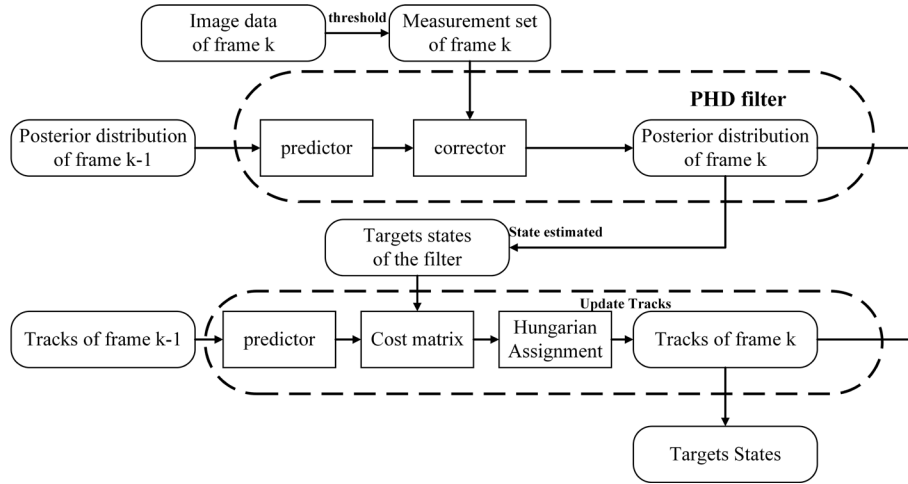


Fig. 4. Schematic diagram of the joint PHD filter and Hungarian assignment algorithm.

generated by the PHD filter. Only if the track survives the trial period will it be considered to be a valid track. Then the current state of the track can be output as the target state. This prevents an unbounded growth of the track number caused by false alarms. Similarly, valid tracks will be terminated only if they are not detected for several frames. This prevents the frequent disappearance of the track caused by the missed detection. Therefore, the proposed algorithm is able to achieve effective target tracking under low SNR. The schematic diagram of the algorithm is shown in Fig. 4.

### 3.2 Thresholding Measurement Set

Suppose that the false alarm probability for processing is  $p_f$ , and the threshold  $\gamma$  for threshold segmentation satisfies

$$p_f = \int_{\gamma}^{+\infty} \mathcal{N}(z; 0, \sigma^2) dz. \quad (20)$$

If the magnitude value  $z_i$  is greater than the threshold  $\gamma$  of pixel  $i = (a, b)$ , the thresholding measurement  $z$  is expressed as the ordered pair of integers  $z = (a, b)$ . The thresholding measurement set  $Z_k = \{z_k^1, \dots, z_k^m\}$  can be obtained by performing threshold segmentation on all  $A \cdot B$  pixels in the image.

In the thresholding measurement set, the mean of false alarm number  $\lambda$  is

$$\lambda = p_f \cdot A \cdot B. \quad (21)$$

This number is used as the mean of the Poisson clutter process in the PHD filter. The detection probability is

$$p_D(\mathbf{x}) = \int_{\gamma}^{+\infty} \mathcal{N}(z_i; h_i(\mathbf{x}), \sigma^2) dz_i. \quad (22)$$

### 3.3 GM-PHD Filter

To improve the computational efficiency, the PHD filter is approximated by the GM implementation. The state vector of the GM PHD filter is denoted by  $\mathbf{y}$  to distinguish it

from the target state vector that the algorithm eventually outputs.

The GM-PHD filter [17] propagates multiple Gaussian components to represent PHD during recursion. At frame  $k$ , the prior PHD is approximately expressed as

$$D_{k-1|k-1}(\mathbf{y}) = \sum_{j=1}^{J_{k-1|k-1}} w_{k-1|k-1}^j \cdot \mathcal{N}(\mathbf{y}; \mathbf{m}_{k-1|k-1}^j, P_{k-1|k-1}^j) \quad (23)$$

where  $J_{k-1|k-1}$  and  $w_{k-1|k-1}^j$  denote the number and weight of the prior Gaussian components, respectively.

The predicted PHD is approximately expressed as

$$D_{k|k-1}(\mathbf{y}) = \sum_{j=1}^{J_{k|k-1}} w_{k|k-1}^j \cdot \mathcal{N}(\mathbf{y}; \mathbf{m}_{k|k-1}^j, P_{k|k-1}^j) \quad (24)$$

where  $J_{k|k-1}$  and  $w_{k|k-1}^j$  denote the number and weight of the predicted Gaussian components, respectively.

Suppose the clutter process can be modelled by a Poisson RFS with mean  $\lambda = p_f \cdot A \cdot B$  and uniform spatial distribution  $c(z)$ , the posterior PHD can be calculated by using the thresholding measurement set  $Z_k$ . After pruning and merging, the posterior PHD is approximately expressed as

$$D_{k|k}(\mathbf{y}) = \sum_{j=1}^{J_{k|k}} w_{k|k}^j \cdot \mathcal{N}(\mathbf{y}; \mathbf{m}_{k|k}^j, P_{k|k}^j) \quad (25)$$

where  $J_{k|k}$  and  $w_{k|k}^j$  denote the number and weight of the Gaussian components, respectively.

The predictor and the corrector of the GM-PHD filter can be found in [17].

The expected number of targets is

$$N_{k|k} = \text{round} \left( \sum_{j=1}^{J_{k|k}} w_{k|k}^j \right). \quad (26)$$

We extract the Gaussian components with the largest  $N_{k|k}$  weights in (25), and the corresponding  $\mathbf{m}_{k|k}^j$  is the state

estimation. Then, in the GM-PHD filter, the multiple target state estimates at frame  $k$  are  $Y_k = \{\hat{y}_k^1, \dots, \hat{y}_k^{N_{k|k}}\}$ .

### 3.4 The Assignment Cost Matrix and Hungarian Assignment Algorithm

The track set at frame  $k-1$  is denoted by  $T_{k-1} = \{\mathbf{t}_{k-1}^1, \dots, \mathbf{t}_{k-1}^{P_{k-1}}\}$ , where  $P_{k-1}$  is the number of tracks and  $l_i$  ( $1 \leq i \leq P_{k-1}$ ) denotes the unique identity of the  $i^{\text{th}}$  track. Then the predicted state of tracks at frame  $k$  is  $\tilde{T}_k = \{\tilde{\mathbf{t}}_k^1, \dots, \tilde{\mathbf{t}}_k^{P_{k-1}}\}$ , in which

$$\tilde{\mathbf{t}}_k^{l_i} = F\mathbf{t}_{k-1}^{l_i}, 1 \leq i \leq P_{k-1} \quad (27)$$

where  $F$  is the state transition matrix.

Since the target state estimates at frame  $k$  are  $Y_k = \{\hat{y}_k^1, \dots, \hat{y}_k^{N_{k|k}}\}$ , the assignment cost matrix is an  $N_{k|k} \times P_{k-1}$  matrix  $C_{N_{k|k} \times P_{k-1}}$  defined as follows:

$$C_{N_{k|k} \times P_{k-1}} = \begin{matrix} c_{1,1} & \cdots & c_{1,j} & \cdots & c_{1,P_{k-1}} \\ \vdots & \ddots & \vdots & \ddots & \vdots \\ c_{i,1} & \cdots & c_{i,j} & \cdots & c_{i,P_{k-1}} \\ \vdots & \ddots & \vdots & \ddots & \vdots \\ c_{N_{k|k},1} & \cdots & c_{N_{k|k},j} & \cdots & c_{N_{k|k},P_{k-1}} \end{matrix} \cdot \quad (28)$$

In SORT, the cost metric is calculated from the bounding box. However, in our work, the targets have no shape at all, and it is impossible to obtain a bounding box. Hence, the assignment cost matrix should be calculated using other parameters.

Here, the element  $c_{i,j}$  in the assignment cost matrix  $C_{N_{k|k} \times P_{k-1}}$  is selected as the Euclidean distance via

$$c_{i,j} = E\{\hat{y}_k^i, \tilde{\mathbf{t}}_k^{l_j}\} \quad 1 \leq i \leq N_{k|k}, 1 \leq j \leq P_{k-1}. \quad (29)$$

Then, the Hungarian assignment algorithm is used to assign the predicted tracks to the target state estimates by using a bipartite graph. The assignment between the target state estimation and the predicted tracks, including the assigned tracks, the unassigned tracks, and the unassigned states, is shown in Sec. 2.3. The sum of the numbers of assigned tracks and unassigned states is  $N_{k|k}$ . The sum of the numbers of assigned tracks and unassigned tracks is  $P_{k-1}$ .

### 3.5 Track Update and Target State Estimate

To update the tracks effectively, 3 counts are defined as follows to distinguish different tracks.  $t_{\text{age}}$ , the age of the track, is used to represent the total frame number from the birth of the track.  $t_{\text{VC}}$ , the total visible count of the track, is used to represent the total frame number the track is esti-

mated by the PHD filter.  $t_{\text{cic}}$ , the consecutive invisible count of the track, is used to represent the frame number the track is continuously missed.

If the tracks at frame  $k-1$  are denoted by  $T_{k-1} = \{\mathbf{t}_{k-1}^1, \dots, \mathbf{t}_{k-1}^{P_{k-1}}\}$ , and the target state estimates at frame  $k$  are  $Y_k = \{\hat{y}_k^1, \dots, \hat{y}_k^{N_{k|k}}\}$ , the tracks at frame  $k$  can be updated according to the assignment as follows.

For the assigned tracks  $(\hat{y}_k^i, \tilde{\mathbf{t}}_k^{l_j})$   $1 \leq i \leq N_{k|k}, 1 \leq j \leq P_{k-1}$ , let the  $i^{\text{th}}$  target state estimates be the state of track  $l_j$  at frame  $k$

$$\mathbf{t}_k^{l_j} = \hat{y}_k^i. \quad (30)$$

We add 1 to the value of the age  $t_{\text{age}}$  and the total visible count  $t_{\text{VC}}$  of the track  $l_j$  and set the value of  $t_{\text{cic}}$  of the track  $l_j$  to 0.

For the unassigned states  $\hat{y}_k^i$  ( $1 \leq i \leq N_{k|k}$ ), we create a new track with a unique identity. Let the unassigned states be the state of the new track at frame  $k$ . Then we set the value of the age  $t_{\text{age}}$  and the total visible count  $t_{\text{VC}}$  of the new track to 1. The value of  $t_{\text{cic}}$  of the new track is set to 0.

For the unassigned tracks  $\tilde{\mathbf{t}}_k^{l_j}$  ( $1 \leq j \leq P_{k-1}$ ), let the predicted state of unassigned tracks be the state of the track at frame  $k$

$$\mathbf{t}_k^{l_j} = \tilde{\mathbf{t}}_k^{l_j}. \quad (31)$$

We add 1 to the value of  $t_{\text{age}}$  and  $t_{\text{cic}}$  of the track  $l_j$  and set a threshold  $\gamma_{\text{cic}}$ . If  $t_{\text{cic}} > \gamma_{\text{cic}}$ , the track  $l_j$  is deleted.

We then set a threshold  $\gamma_{\text{tvc}}$ . In the updated track, if the total visible count  $t_{\text{tvc}} \geq \gamma_{\text{tvc}}$ , the track is determined to be a valid track and the state of the tracks is output as the target state estimate of the proposed algorithm. To achieve effective target tracking under low SNR, a valid track will be terminated only if  $t_{\text{tvc}} \geq \gamma_{\text{tvc}}$ . This prevents the frequent disappearance of the track caused by the missed detection. Therefore, the proposed algorithm will generate a certain delay of the tracking when the target number changes.

If the number of valid tracks of the proposed algorithm is  $n$ , the estimated target states can be expressed as  $X_k = \{\mathbf{x}_k^1, \dots, \mathbf{x}_k^n\}$ . The pseudocode is shown in Algorithm 1.

Algorithm 1 Pseudocode of joint PHD filter and Hungarian assignment algorithm

1. Input: Image
2. Obtain  $Z_k$  by performing threshold segmentation
3. Calculate  $\lambda$  and  $p_D(\mathbf{x})$
4. Predictor and corrector of the GM-PHD filter
5. Estimate target number  $N_{k|k}$  and states  $Y_k = \{\hat{y}_k^1, \dots, \hat{y}_k^{N_{k|k}}\}$
6. Calculate the assignment cost matrix  $C_{N_{k|k} \times P_{k-1}}$
7. Obtain the assigned tracks, the unassigned tracks, and the unassigned states by using Hungarian assignment algorithm
8. Tracks update
9. Target state estimate
10. Output: Estimate of target state:  $X_k = \{\mathbf{x}_k^1, \dots, \mathbf{x}_k^n\}$

### 3.6 Analysis of the Computational Complexity

The PHD filter has a computational complexity of  $O(mn)$ , where  $m$  represents the number of thresholding measurements and  $n$  represents the number of targets. We utilize the Hungarian assignment algorithm to assign predicted tracks to target state estimates, with both being approximately equal to the number of targets. Therefore, the computational complexity of the Hungarian assignment algorithm is solely dependent on the target number and not the measurement number. In the worst case, the computational complexity of the Hungarian algorithm is  $O(n^3)$ , but typically it is much lower, sometimes even achieving a linear computational complexity. In the tracking scene in low SNR in our work, the target number  $n$  is much smaller than the thresholding measurement number  $m$ . So even compared to that of the PHD filter ( $O(mn)$ ), the computational complexity of the Hungarian assignment algorithm is much smaller. Therefore, the joint PHD filter and Hungarian assignment algorithm proposed in this work has a computational complexity slightly greater than  $O(mn)$ .

As a provable Bayes optimal tracking filter, the GLMB filter has higher complexity than the PHD filter. If each component of the predicted density using Murty's algorithm to find the  $K$  most significant components in the calculation of the measurement update, the computational complexity of the GLMB filter is  $O(k(n+m)^3)$  [23]. Using the Gibbs sampling to replace the Murty's algorithm, the computational complexity of the fast implementation of the GLMB filter is  $O(kn^2m)$  [25]. Hence, the proposed algorithm is more efficient than the GLMB filter and its implementation is fast.

## 4. Simulation

### 4.1 Setup of Simulation

The targets in our work are modelled as points with state variables  $\mathbf{x}_k = [x_k, \dot{x}_k, y_k, \dot{y}_k]^T$ , where  $(x_k, y_k)$  denotes the

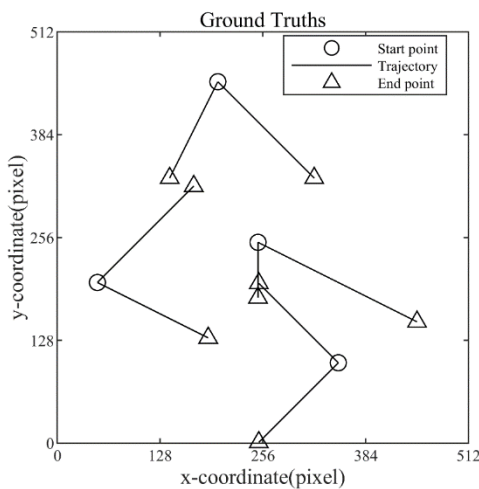


Fig. 5. Ground truth of targets.

target position at frame  $k$ , and  $(\dot{x}_k, \dot{y}_k)$  denotes the target velocity at frame  $k$ . A constant velocity (CV) model [29] with sampling period  $T = 0.04$  s is used. The simulations continue for 4 seconds with 100 frames. The state transition model is

$$\mathbf{x}_k = F\mathbf{x}_{k-1} + G\mathbf{w}_{k-1}, \quad (32)$$

$$F = I_2 \otimes \begin{bmatrix} 1 & T \\ 0 & 1 \end{bmatrix}, G = \begin{bmatrix} \frac{T^2}{2} & T & 0 & 0 \\ 0 & 0 & \frac{T^2}{2} & T \end{bmatrix}^T \quad (33)$$

where  $\mathbf{w}_{k-1} = [w_{x,k-1}, w_{y,k-1}]^T$  represents the noise components with standard deviations  $\sigma_x = \sigma_y = 5$  pixel/s<sup>2</sup>.  $I_2$  is a  $2 \times 2$  identity matrix and  $\otimes$  represents the Kronecker product.

The dynamic scenario for simulation is shown in Tab. 1 and Fig. 5. In the state  $\mathbf{x}_k = [x_k, \dot{x}_k, y_k, \dot{y}_k]^T$  shown in Tab. 1, the unit of  $(x_k, y_k)$  is pixel, and the unit of  $(\dot{x}_k, \dot{y}_k)$  is pixel/s.

A common observation model with the two-dimensional observation image consists of an array of pixels with scalar magnitude values is simulated in this section, as defined in Sec. 2.4. The observation image is a 512 pixel  $\times$  512 pixel array, with array indices represented

Target	Initial state	Appearance	Disappearance
1	[250,0,250,-25]	1	71
2	[350,-25,100,25]	1	Not disappear
3	[50,50,200,-25]	1	71
4	[350,-25,100,-25]	1	Not disappear
5	[250,50,250,-25]	1	Not disappear
6	[200,50,450,-50]	40	Not disappear
7	[50,50,200,50]	40	Not disappear
8	[200,-25,450,-50]	40	Not disappear

Tab. 1. Target motion parameters for simulation.

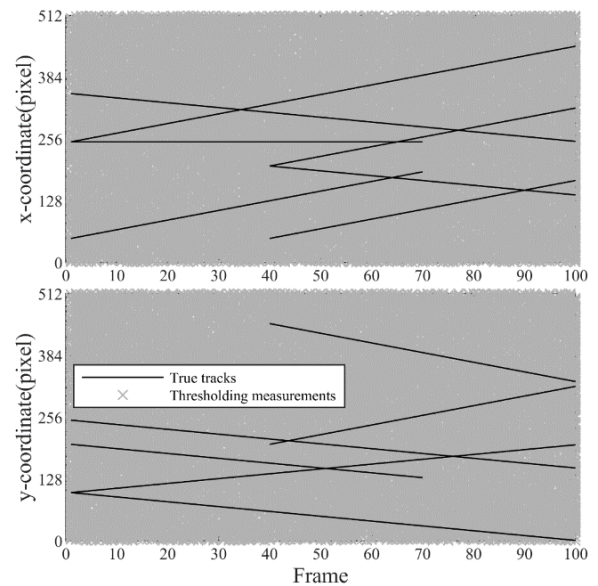


Fig. 6. True tracks and the thresholding measurements.

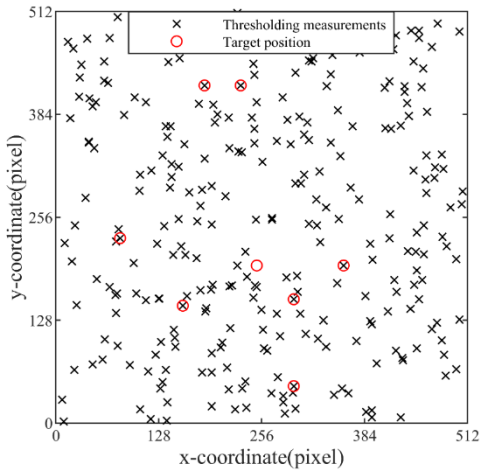


Fig. 7. Thresholding measurements and target position of frame 55.

as ordered pair of integers  $(x,y)$ . The targets used in the simulation are point targets. For regions outside their influence, the PDF of the background magnitude values follows a Gaussian density with a zero mean and standard deviation  $\sigma = 500$ . The SNR for the simulation image is set to 4, making it challenging to detect the point targets. In the threshold segmentation, to obtain a high target detection probability, the false alarm probability for processing is  $p_f = 0.001$ . In this case, the target detection probability is  $p_D = 0.8185$ . Then, the mean number of false alarms in each frame is approximately 262. The thresholding measurements are shown in Fig. 6.

To provide a clearer representation of the target and thresholding measurements, Figure 7 displays the thresholding measurements and target position for frame 55. There are 8 real targets in the figure, but due to the low SNR, there is one target (target 1) that does not produce measurement. That is, the target 1 is missed. The number of false alarms in the figure is 275, and it can be seen that the number of false alarms is very large. The figures show that the false alarms are very dense, which might reduce the tracking performance and increase the computational complexity of the tracking filters.

In the joint PHD filter and Hungarian assignment algorithm, the threshold for deleting the track is selected as  $\gamma_{cic} = 10$ , and the threshold to determine the track as a valid track is selected as  $\gamma_{tvc} = 4$ .

### 4.2 Simulation Results

Figure 8 depicts the tracking results achieved with the proposed algorithm, compared against the classical PHD filter without association. It can be seen from the figure that due to the large number of false alarms and the missed detection of the targets, it is easy to obtain wrong tracking results by using the PHD filter. However, with the Hungarian assignment algorithm, the proposed algorithm can correctly estimate the state of the target even though the number of false alarms is large. This is because the incorrect tracking

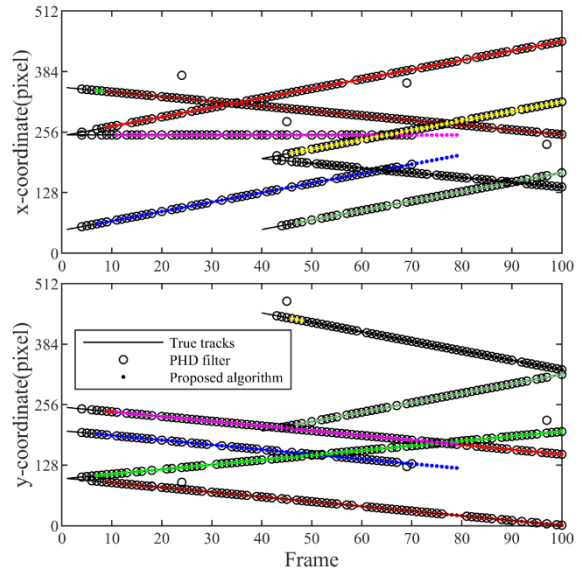


Fig. 8. The tracking results.

results do not reach the threshold for judging the appearance or disappearance of the target. Thus, the estimation of the target state is more accurate in low SNR.

Figure 9 shows the estimated target number of our algorithm. Due to a large number of false alarms and missed detections, the estimated target number of the PHD filter is lower than the true number of the targets most of the time. With the Hungarian assignment algorithm, the estimated target number of the proposed algorithm is consistent with the true target number, except for the few frames in which the targets have just appeared. This shows that the proposed algorithm can estimate the target number correctly in low SNR.

Figure 10 shows the optimal subpattern assignment (OSPA) metric [30] of the target state estimation obtained by the proposed algorithm. The parameters of the OSPA metric are selected as  $p = 2$  and  $c = 3$  pixel. Although the target state is predicted from the state at the previous moment when the target is missed by the PHD filter, the OSPA metric of the proposed algorithm is still small. Compared with the PHD filter, the tracking error of the proposed algorithm is much smaller except for a few frames after the target number changes. This shows that the proposed algorithm has better tracking performance than the PHD filter in low SNR.

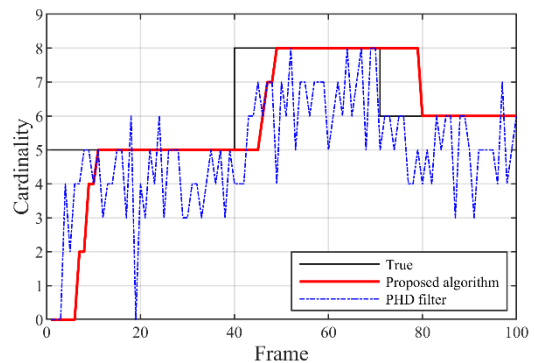


Fig. 9. The estimated target number of the proposed algorithm.

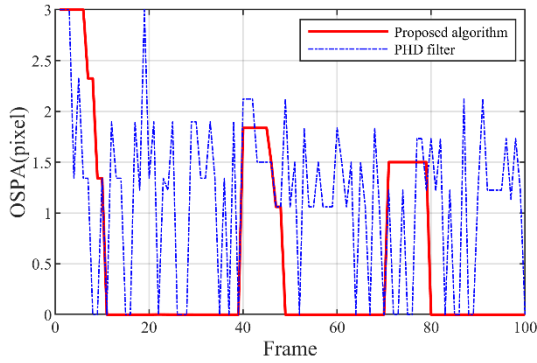


Fig. 10. The OSPA metric of the proposed algorithm.

### 4.3 Tracking Performance and Computational Complexity of the Algorithm

To fully illustrate the tracking performance of the proposed algorithm in low SNR, we simulate the average tracking performance of the proposed algorithm with 1000 Monte Carlo simulations. The fast implementation of the GLMB filter [24], [25], which is the best-performing filter within the RFS framework, is used as a comparison algorithm. The estimated target numbers of the PHD filter, the GLMB filter, and our algorithm are shown in Fig. 11. It can be seen that the average target number estimated by the PHD filter is lower than the true number of targets. The average target numbers estimated by our algorithm and the GLMB filter are consistent with the true number of the targets, except for a few frames after the target number changes. This further illustrates that our algorithm can estimate the target number correctly in low SNR.

Figure 12 shows the average OSPA metric of the target state estimation by 1000 Monte Carlo simulations. It can be seen that the average OSPA metric of our algorithm is much smaller than that of the PHD filter. At the same time, the average OSPA metric of our algorithm is smaller than that of the GLMB filter, except for a few frames after the target number changes.

Since our algorithm is a tracking algorithm with tracking label, the  $OSPA^{(2)}$  metric [31] needs to be used to evaluate its labeled tracking performance. The average  $OSPA^{(2)}$  metric of our algorithm is shown in Fig. 13. Only the GLMB

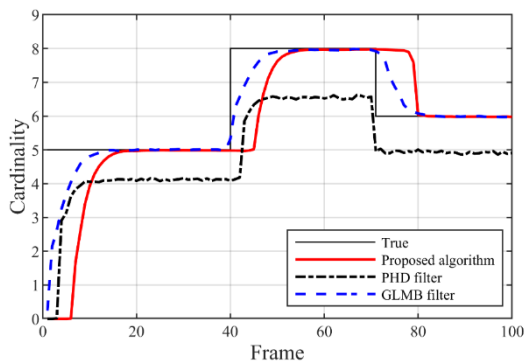


Fig. 11. The average estimated target number.

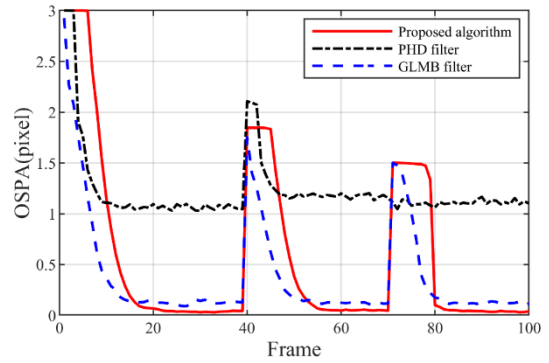


Fig. 12. The average OSPA metric.

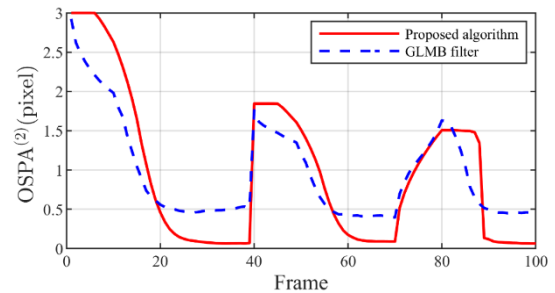


Fig. 13. The average  $OSPA^{(2)}$  metric.

filter is used as the comparison algorithm, because the PHD filter is not a tracking algorithm with tracking label. It can be seen that the average  $OSPA^{(2)}$  metric of our algorithm is smaller than that of the GLMB filter, except for a few frames after the target number changes. Thus, from the point of view of the entire tracking process, it can be considered that the tracking performance of the proposed algorithm is comparable to that of the GLMB filter. In fact, the GLMB filter is the best-performing filter within the RFS framework. Therefore, we can conclude that our algorithm has good tracking performance in low SNR.

Despite good tracking performance, the GLMB filter also suffers from high computational complexity due to the use of a labeled multi-Bernoulli RFS to approximate the posterior PDF. However, the computational complexity of our algorithm is low because the PHD filter is used to complete the filtering and the Hungarian assignment algorithm is used to complete the track assignment. Figure 14 shows the average calculation time of each frame of our algorithm. It can be seen from the figure that the computation time of the algorithm has almost no increase compared with the PHD filter. This is because the number of target states generated by the PHD filter is relatively small, and the computational complexity for the assignment algorithm is very small. However, since the GLMB filter does not have the similar computational advantages of the PHD filter, its computational complexity is much higher than that of the PHD filter and our algorithm. As seen from the figure, the computation time of each frame of our algorithm is less than 0.04 s, which is shorter than the frame period used in the simulation. Thus, our algorithm can be implemented in real time. However, the computation time of the GLMB filter is greater than 0.08 s, which means that the GLMB filter cannot be implemented

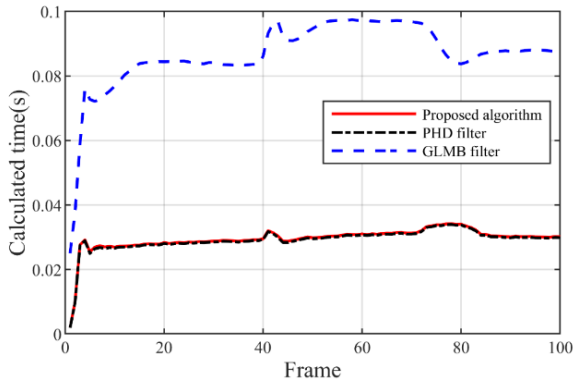


Fig. 14. Average calculation time of each frame.

in real time. Therefore, although the performance of the GLMB filter is comparable to that of the proposed algorithm, it is not suitable for target tracking scenarios that need to be implemented in real time.

Therefore, the algorithm proposed in this paper is a high-performance target tracking algorithm that can be implemented quickly in low SNR.

## 5. Conclusion and Future Work

This paper presents a novel approach to achieving real-time MTT in low SNR by utilizing a joint PHD filter and Hungarian assignment algorithm. The PHD filter is used for preliminary tracking of targets, and the Hungarian assignment algorithm is used to complete the association. The simulation results show that the proposed tracking algorithm can achieve stable multitarget tracking in low SNR with small computational complexity. In the future, the proposed algorithm should be transplanted from the computer in order to the embedded system to improve the MTT performance in low SNR.

## Acknowledgments

This work was supported by the National Natural Science Foundation of China (61901489).

## References

[1] EBENEZER, S., PAPANDREOU-SUPPAPPOLA, A. Generalized recursive track-before-detect with proposal partitioning for tracking varying number of multiple targets in low SNR. *IEEE Transactions on Signal Processing*, 2016, vol. 64, no. 11, p. 2819–2834. DOI: 10.1109/TSP.2016.2523455

[2] RICHARDS, M. *Fundamentals of Radar Signal Processing*. 1<sup>st</sup> ed. New York (USA): McGraw-Hill, 2005. ISBN: 9780070607378

[3] RISTIC, B., ARULAMPALAM, S., GORDON, N. *Beyond the Kalman Filter: Particle Filters for Tracking Applications*. Norwood (USA): Artech House, 2004. ISBN: 9781580536318

[4] BARNIV, Y. Dynamic programming solution for detecting dim moving targets. *IEEE Transactions on Aerospace and Electronic Systems*, 1985, vol. 21, no. 1, p. 144–156. DOI: 10.1109/TAES.1985.310548

[5] BO, J., YU, H., WANG, G. The HT-TBD algorithm for large maneuvering targets with fewer beats and more groups. In *Proceedings of IEEE 4th Advanced Information Management, Communicates, Electronic and Automation Control Conference (IMCEC)*. Chongqing (China), 2021, p. 202–206. DOI: 10.1109/IMCEC51613.2021.9482140

[6] ELHOSHY, M., GEBALI, F., GULLIVER, T. Expanding window dynamic-programming-based track-before-detect with order statistics in Weibull distributed clutter. *IEEE Transactions on Aerospace and Electronic Systems*, 2020, vol. 56, no. 4, p. 2564–2575. DOI: 10.1109/TAES.2019.2948451

[7] TONISSEN, S., BAR-SHALOM, Y. Maximum likelihood track-before-detect with fluctuating target amplitude. *IEEE Transactions on Aerospace and Electronic Systems*, 1998, vol. 34, no. 3, p. 796 to 809. DOI: 10.1109/7.705887

[8] SU, H., WU, T., LIU, H., et al. Rao-Blackwellised particle filter based track-before-detect algorithm. *IET Signal Processing*, 2008, vol. 2, no. 2, p. 169–176. DOI: 10.1049/iet-spr:20070075

[9] CLARK, D., RISTIC, B., VO, B.-N., et al. Bayesian multi-object filtering with amplitude feature likelihood for unknown object SNR. *IEEE Transactions on Signal Processing*, 2010, vol. 58, no. 1, p. 26–37. DOI: 10.1109/TSP.2009.2030640

[10] YANG, B., WANG, J., YUAN, C., et al. Multi-object Bayesian filters with amplitude information in clutter background. *Signal Processing*, 2018, vol. 152, p. 22–34. DOI: 10.1016/j.sigpro.2018.05.004

[11] DU, R., LIU, L., BAI, X., et al. A new scatterer trajectory association method for ISAR image sequence utilizing multiple hypothesis tracking algorithm. *IEEE Transactions on Geoscience and Remote Sensing*, 2022, vol. 60, p. 1–13. DOI: 10.1109/TGRS.2021.3087192

[12] HE, S., SHIN, H., TSOURDOS, A. Distributed multiple model joint probabilistic data association with Gibbs sampling-aided implementation. *Information Fusion*, 2020, vol. 64, p. 20–31. DOI: 10.1016/j.inffus.2020.04.007

[13] MAHLER, R. *Statistical Multisource Multitarget Information Fusion*. Norwood (USA): Artech House, 2007. ISBN: 978-1596930926

[14] MAHLER, R. *Advances in Statistical Multisource-Multitarget Information Fusion*. Norwood (USA): Artech House, 2014. ISBN: 9781608077984

[15] MAHLER, R. Multitarget Bayes filtering via first-order multitarget moments. *IEEE Transactions on Aerospace and Electronic Systems*, 2003, vol. 39, no. 4, p. 1152–1178. DOI: 10.1109/TAES.2003.1261119

[16] VO, B.-N., SINGH, S., DOUCET, A. Sequential Monte Carlo methods for multi-target filtering with random finite sets. *IEEE Transactions on Aerospace and Electronic Systems*, 2005, vol. 41, no. 4, p. 1224–1245. DOI: 10.1109/TAES.2005.1561884

[17] VO, B.-N., MA, W.-K. The Gaussian mixture probability hypothesis density filter. *IEEE Transactions on Signal Processing*, 2006, vol. 54, no. 11, p. 4091–4104. DOI: 10.1109/TSP.2006.881190

[18] PANTA, K., VO, B.-N., SINGH, S. Novel data association schemes for the probability hypothesis density filter. *IEEE Transactions on Aerospace and Electronic Systems*, 2007, vol. 43, no. 2, p. 556–570. DOI: 10.1109/TAES.2007.4285353

[19] XIAO, H., LI, Y., FU, Q. Identification and tracking of towed decoy and aircraft using multiple-model improved labeled P-PHD filter. *Digital Signal Processing*, 2015, vol. 46, p. 49–58. DOI: 10.1016/j.dsp.2015.07.005

- [20] WANG, S., BAO, Q., CHEN, Z. Refined PHD filter for multi-target tracking under low detection probability. *Sensors*, 2019, vol. 19, no. 13, p. 1–17. DOI: 10.3390/s19132842
- [21] VO, B.-T., VO, B.-N. Labeled random finite sets and multi-object conjugate priors. *IEEE Transactions on Signal Processing*, 2013, vol. 61, no. 13, p. 3460–3475. DOI: 10.1109/TSP.2013.2259822
- [22] REUTER, S., VO, B.-T., VO, B.-N., et al. The labeled multi-Bernoulli filter. *IEEE Transactions on Signal Processing*, 2014, vol. 62, no. 12, p. 3246–3260. DOI: 10.1109/TSP.2014.2323064
- [23] VO, B.-N., VO, B.-T., PHUNG, D. Labeled random finite sets and the Bayes multi-target tracking filter. *IEEE Transactions on Signal Processing*, 2014, vol. 62, no. 24, p. 6554–6567. DOI: 10.1109/TSP.2014.2364014
- [24] KROPFREITER, T., MEYER, F., HLAWATSCH, F. A fast labeled multi-Bernoulli filter using belief propagation. *IEEE Transactions on Aerospace and Electronic Systems*, 2020, vol. 56, no. 3, p. 2478 to 2488. DOI: 10.1109/TAES.2019.2941104
- [25] VO, B.-N., VO, B.-T., HOANG, H. An efficient implementation of the generalized labeled multi-Bernoulli filter. *IEEE Transactions on Signal Processing*, 2017, vol. 65, no. 8, p. 1975–1987. DOI: 10.1109/TSP.2016.2641392
- [26] BEWLEY, A., GE, Z., OTT, L., et al. Simple online and realtime tracking. In *Proceedings of 2016 IEEE International Conference on Image Processing (ICIP)*. Phoenix (USA), 2016, p. 3464–3468. DOI: 10.1109/ICIP.2016.7533003
- [27] KUHN, H. The Hungarian method for the assignment problem. *Naval Research Logistics*, 1955, vol. 2, p. 83–97. DOI: 10.1007/978-3-540-68279-0\_2
- [28] WOJKE, N., BEWLEY, A., PAULUS, D. Simple online and realtime tracking with a deep association metric. In *Proceedings of 2017 IEEE International Conference on Image Processing (ICIP)*. Beijing (China), 2017, p. 3645–3649. DOI: 10.1109/ICIP.2017.8296962
- [29] LI, X. R., JILKOV, V. P. Survey of maneuvering target tracking: Part I. Dynamic models. *IEEE Transactions on Aerospace and Electronic Systems*, 2003, vol. 39, no. 4, p. 1333–1364. DOI: 10.1109/TAES.2003.1261132
- [30] SCHUHMACHER, D., VO, B.-T., VO, B.-N. A consistent metric for performance evaluation of multi-object filters. *IEEE Transactions on Signal Processing*, 2008, vol. 56, no. 8, p. 3447–3457. DOI: 10.1109/TSP.2008.920469
- [31] BEARD, M., VO, B.-T., VO, B.-N. OSPA<sup>(2)</sup>: Using the OSPA metric to evaluate multi-target tracking performance. In *Proceedings of 2017 International Conference on Control, Automation and Information Sciences (ICCAIS)*. Chiang Mai (Thailand), 2014, p. 86–91. DOI: 10.1109/ICCAIS.2017.8217598

## About the Authors ...

**Shanzhu XIAO** was born in 1978. He received his M.S. degree from the National University of Defense Technology (NUDT), Changsha, China, in 2002. He is currently a researcher at the National Key Laboratory of Science and Technology on Automatic Target Recognition, NUDT. His research interests include automatic target recognition, integrated circuit and real time system.

**Huamin TAO** was born in 1972. She received her M.S. degree from the NUDT, Changsha, China, in 1997. She is currently a researcher at the National Key Laboratory of Science and Technology on Automatic Target Recognition, NUDT. Her research interests include signal processing and real-time system design.

**Xinglin SHEN** (corresponding author) was born in 1990. He received the B.S. degree from the South China University of Technology (SCUT) in 2012, and the M.S. and Ph.D. degrees from the NUDT in 2014 and 2018, respectively. He is currently a Lecturer with the National Key Laboratory of Science and Technology on ATR, College of Electronic Science, NUDT. His research interests include signal processing, target detection and tracking, and Bayesian filtering.

**Luping ZHANG** was born in 1985. He received the M.S. and Ph.D. degrees in Information and Communication Engineering from the NUDT in 2010 and 2015, respectively. He is currently an Associate Researcher with the College of Electronic Science and Engineering. His research interests include object detecting, pattern recognition, and visual tracking.

**Moufa HU** was born in Hubei, China, in 1979. He received the B.S., M.S., and Ph.D. degrees from the NUDT, in 2001, 2003, and 2008, respectively. He is now an Associate Researcher with the National Key Laboratory of Science and Technology on Automatic Target Recognition, University of Defense Science and Technology, Changsha. He has authored or coauthored more than 40 journal and conference proceedings papers. He has been the principal investigator of 20 research projects. His research interests include optical imaging target detection and recognition, intelligent image real-time information processing, and algorithm performance evaluation.